Specific anion effect on properties of HRV 3C protease

Eva Dušeková[1,⁋], Martin Berta[1,⁋], Dagmar Sedláková[2,⁋], David Řeha[3], Veronika Dzurillová[1], Anastasiia Shaposhnikova[3,4], Fatemeh Fadaei[3,4], Mária Tomková[5], Babak Minofar[3*], Erik Sedlák[5*]

[1]Department of Biophysics, Faculty of Science, P. J. Šafárik University in Košice, Jesenná 5, 04154 Košice, Slovakia

[2]Department of Biophysics, Institute of Experimental Physics, Slovak Academy of Sciences, Watsonova 47, 040 01 Košice, Slovakia

[3]Faculty of Science, University of South Bohemia in České Budějovice, Branišovská 1645/31A, 37005 České Budějovice, Czech Republic.

[4]Laboratory of Structural Biology and Bioinformatics, Institute of Microbiology of the Czech Academy of Sciences, Zámek 136, 37333 Nové Hrady, Czech Republic

[5]Centre for Interdisciplinary Biosciences, P. J. Šafárik University in Košice, Jesenná 5, 04154 Košice, Slovakia

⁋ The authors contributed equally to this work

[*] To whom correspondence should be addressed:

Faculty of Science, University of South Bohemia, Branišovská 1760, 37005 České Budějovice, Czech Republic; email: babakminoofar@gmail.com

Centre for Interdisciplinary Biosciences, P. J. Šafárik University in Košice, Jesenná 5, 04154 Košice, Slovakia; email: erik.sedlak@upjs.sk

Abstract

Specific salts effect is intensively studied from the prospective of modification of different physico-chemical properties of biomacromolecules. Limited knowledge of the specific salts effect on enzymes led us to address the influence of five sodium anions: sulfate, phosphate, chloride, bromide, and perchlorate, on catalytic and conformational properties of human rhinovirus-14 (HRV) 3C protease. The enzyme conformation was monitored by circular dichroism spectrum (CD) and by tyrosines fluorescence. Stability and flexibility of the enzyme have been analyzed by CD in the far-UV region, differential scanning calorimetry and molecular dynamics simulations, respectively. We showed significant influence of the anions on the enzyme properties in accordance with the Hofmeister effect. The HRV 3C protease in the presence of kosmotropic anions, in contrast with chaotropic anions, exhibits increased stability, rigidity. Correlations of stabilization effect of anions on the enzyme with their charge density and the rate constant of the enzyme with the viscosity B-coefficients of anions suggest direct interaction of the anions with HRV 3C protease. The role of stabilization and decreased fluctuation of the polypeptide chain of HRV 3C protease on its activation in the presence of kosmotropic anions is discussed within the frame of the macromolecular rate theory.

Keywords: Hofmeister effect; enzyme activation; cysteine protease

1. Introduction

Solvent surrounding proteins inevitably affects their physico-chemical properties such as stability and dynamics of protein structure and their interfacial properties [1–3]. Increased ionic strength **(>0.3 M)** of the solvent by different inorganic salts is one of the simplest but very intensively studied way of modification of aqueous solvent properties. This so-called Hofmeister effect is a matter of interest of numerous studies due to an effort to understand how ion hydration and protein-ion interactions modulate conformational, colloidal and functional properties of proteins/enzymes. Indeed, the salt composition of solvent significantly affects number of biophysical and biochemical processes including protein stability [4–6], colloidal stability and fibrillization [7–9], enzymatic activity [10–13] and many others [14–16]. Ion specific effect have been observed even at low salt concentrations indicating more specific protein-ion interaction [9,13]. However, aqueous high ionic strength conditions are attractive from biotechnological point of view because utilization such production conditions significantly reduces expenses related with sterilization and necessity to employ expensive materials for fermentation facilities [17]. An exotic branch of the research is related to the effect of high salinity in combination with other physical and chemical factors such as temperature, pressure, and pH on enzymes in connection with habitability of extraterrestrial bodies with prime candidate Mars [18] on which surface perchlorate salts and sulfates have been detected [19,20].

For systematic analysis of the specific salt effect on enzyme properties, we chose human rhinovirus-14 (HRV) 3C protease or **PreScission™**. This selection was made for the following reasons: (i) it has been reported that HRV 3C protease can be activated by kosmotropic salts [21,22], but in these reports, the Hofmeister effect has not been systematically exploited in regards kinetic and conformational parameters of the enzyme, (ii) effect of kosmotropic and chaotropic anions can be clearly distinguished from each other, providing thus opportunities for correlating modulated properties of HRV 3C protease with the inherent properties of anions, and (iii) perspective utilization of HRV 3C protease in recombinant protein production for pharmaceutical and biotechnological applications [23]. Human rhinovirus, the most frequent causative agent of the common cold, is the members of the picornavirus family and HRV 3C protease is responsible for processing of the viral polyprotein. Noteworthy, HRV 3C protease is homologous with the 3-chymotrypsin-like cysteine (3CLpro) protease of severe acute respiratory syndrome coronavirus 2 (SARS-CoV-

2), which is considered a major target for the discovery of direct antiviral agents [24]. The HRV 3C protease consists of 182 amino acids, contains no tryptophan and four tyrosines and its isoeletric point is ~8.5. This cysteine protease folds into two topologically equivalent six-stranded β barrels and in this sense is similar to chymotrypsin-like cysteine protease with the catalytic triad composed of His40-Glu71-Cys146, positioned in analogous way as in serine proteases [25]. The optimum substrate recognition motif for HRV 3C protease is ETLGQ/GP [26,27], for comparison, the preferred P2–P1–P1' substrate sequence for 3CLpro is LQ/(S, A, G) [28]. The catalytic mechanism of the HRV 3C protease has been recently comprehensively analyzed and its simplified version is presented in the Scheme 1 [29].

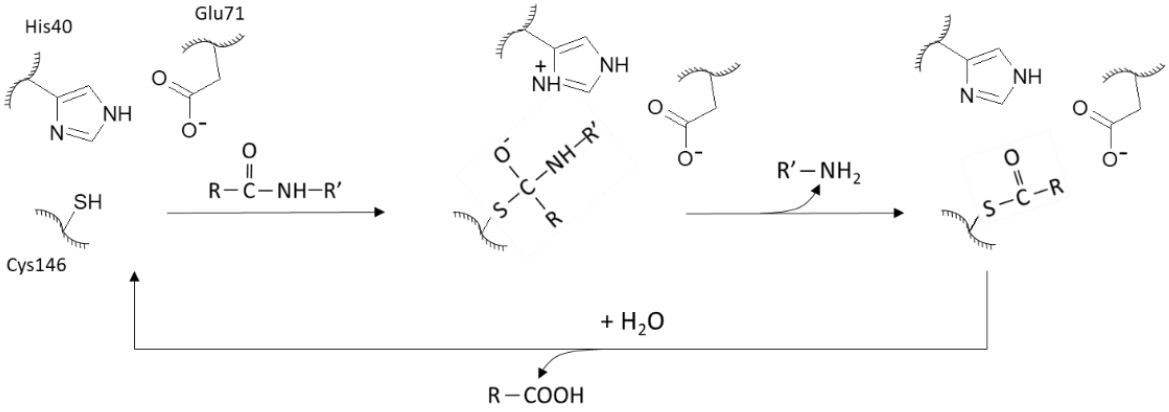

Scheme 1. General scheme of HRV 3C protease. The catalytic mechanism of the cysteine protease is analogous to that of the serine protease in which the nucleofilic serine is replaced by the cysteine [29].

Obtained results clearly shows close correlation between inherent properties of anions such as charge density and B-viscosity coefficient with conformational and catalytic properties of HRV 3C protease. We show that increased stability and the rigidity of the polypeptide chain of HRV 3C protease is accompanied with its increased catalytic activity. This conclusion is in agreement with the recent macromolecular rate theory [30], consistent with the classical description of the enzyme catalysis, according which an enzyme tightly binds the transition state.

2. Materials and methods

Salts $Na_2HPO_4.2H_2O$, $NaH_2PO_4.H_2O$, NaCl, and $NaClO_4.H_2O$ and buffers citrate phosphate, MOPS (3-(N-morpholino)propanesulfonic acid), HEPES, glycine and PBS (phosphate buffered-saline) were purchased from Sigma Aldrich. NaBr was obtained from

Penta, Na_2SO_4 from Merck. Substrate for the enzyme assay, pentapeptide Glu-Ala-Leu-Phe-Gln conjugated to the chromogenic p-nitroanilide (pNA) through the amide bond (EALFQ-pNA), has been obtained from ThermoFischer with purity higher than 95%.

2.1. Enzyme expression and purification

The HRV 3C protease (EC 3.4.22.28) expression and purification have been performed as previously described [31]. In brief, the enzyme was expressed in the *E. coli* strain BL21 in 2xYT medium containing 35 µg/ml kanamycin and 0.4% glucose. Protein expression at 37°C was induced with 1 mM IPTG upon reaching OD600 ~0.6 and continued for the next 4 hours. After incubation, the cells were harvested by centrifugation and frozen in liquid nitrogen till they were further proceeded.

All the purification steps were carried out on the ice and with cooled (4°C) buffers. The cell pellet was resuspended in TBS lysis buffer pH 8.0 (4 ml/g) containing 50 mM Tris-HCl, 400 mM NaCl and lysozyme (1.5 mg/ml). The cells were disrupted using sonification and cell debris was removed by centrifugation. The filtrated supernatant was applied to a pre-equilibrated IMAC column (Ni-NTA Superflow resin, Qiagen) and washed with 10 column volumes (CV) of TBS washing buffer pH 8.0 (50 mM Tris-HCl, 400 mM NaCl pH, 20 mM imidazole and 10% glycerol), 10 CV of TBS low-salt buffer pH 8.0 (50 mM Tris-HCl, 20 mM NaCl, 20 mM imidazole and 10% glycerol), 10 CV of TBS high-salt buffer pH 8.0 (50 mM Tris-HCl, 1 M NaCl pH, 20 mM imidazole and 10% glycerol) and again 10 CV of TBS washing buffer. Finally, the proteins were eluted with TBS elution buffer pH 7.4 (50 mM Tris-HCl, 400 mM NaCl pH, 250 mM imidazole and 10% glycerol), frozen in liquid nitrogen and stored at -80°C.

2.2. Enzyme assays of activity of HRV 3C protease

Kinetic measurements were performed on UV-VIS absorption spectrophotometer Specord S300 equipped by Peltier element (Analytic Jena). The concentration of HRV 3C protease was determined from the absorbance at 280 nm and an extinction coefficient of 6085 $M^{-1}cm^{-1}$ [32]. The rate of HRV 3C protease-catalyzed substrate hydrolysis was measured by following the increase in absorbance at 410 nm due to a release of a free pNA. The temperature during all measurements was kept constant at 25 °C. Data were collected for 2 minutes from the start of the reaction. The initial reaction velocities were determined from the slope of the initial increase in the absorbance at the 410 nm. The absorbance was converted to molar concentration using molar extinction coefficient for pNA of 8800 $M^{-1}cm^{-1}$ at 410 nm. The measurements were performed in the presence of five sodium salts at four different concentrations (0.25 M, 0.5 M, 0.75 M and 1 M). The solvents with the different salt

concentrations were prepared by mixing of the corresponding 1M salt in 20 mM HEPES, pH 7.8 and 20 mM HEPES, pH 7.8. The stability of pH values of the salt solutions was controlled before and after all measurements. Before each measurement, the buffer solution along with the enzyme was incubated for 10 minutes at 25 °C. The reaction was started by adding EALFQ-pNA, with final concentrations in the range from 20 μM to 150 μM. Experimentally determined data were fitted according to Michaelis-Menten equation:

$$v = V_{max}\frac{[S]}{K_M + [S]} \qquad (1)$$

where V_{max} is the maximal velocity, [S] is the substrate concentrations and K_M is the Michaelis constant.

2.3. Dependences of catalytic activity on pH

The pH activity of HRV 3C protease was measured in the presence of 250 μM of the substrate in the effort to achieve the high occupancy of the active site of the enzyme by the substrate. The activity of HRV 3C protease was measured in the pH range 4.0-7.5 in 20 mM citrate-phosphate buffer, in the pH range 6.5-8.0 in 20 mM MOPS, in the pH range 8.0-10.0 in 20 mM glycine buffer, and at pH 7.8 in PBS buffer and in 20 mM HEPES.

The value of pK_a of the catalytic activity of HRV 3C protease on pH was determined using the following equation:

$$S = \frac{S_N + m_N.pH + (S_D + m_D.pH)10^{n(pK_a - pH)}}{1 + 10^{n(pK_a - pH)}} \qquad (2)$$

where S is the observed parameter represented by either ellipticity at 218 nm or the normalized enzyme activity, S_N and S_D are the intercepts of linear dependences of the followed parameters before and after the transition, respectively. The values m_N and m_D refer to slopes of the linear dependences of the followed parameters before and after the transition, respectively. The pH values were measured directly in the cuvettes using a Sensorex glass microelectrode.

2.4. Circular dichroism spectrum of HRV 3C protease

Circular dichroism (CD) spectra of HRV 3C protease in the far-UV and in the near-UV spectral region were performed with spectropolarimeter Jasco J-815 using a 1 mm and 5 mm path-length quartz cuvette, respectively, at 25°C. The temperature was controlled with a Peltier block CDF-426S/15. The spectra are the average of 8 consecutive scans, recorded with a scan rate of 50 nm/min and bandwidth of 1 nm. The protein concentration was 30 μM.

Measurements were performed in 20 mM HEPES, pH 7.8, in the absence and in the presence of 1 M salts.

The pH dependence of the secondary structure of HRV 3C protease was measured by collecting spectra in the far-UV spectral region. The pH of the solvent was changed by an addition of HCl or NaOH and the pH values were measured directly in the cuvettes using a Sensorex glass microelectrode (before and after recording spectra).

2.5. Thermal stability of HRV 3C protease (circular dichroism and differential scanning calorimetry)

Circular dichroism. Thermal denaturation of HRV 3C protease was obtained by monitoring the ellipticity at a single wavelength in dependence on temperature. The ellipticity signal at given temperature has been collected for 16 s with the step of 0.5°C. The measurements of thermal denaturation of HRV 3C protease in the presence of phosphate buffer, $NaClO_4$, NaCl, and Na_2SO_4, were performed by monitoring the CD signal at 210 nm and in the presence of NaBr, due to its high absorbance below 230 nm, the CD signal was monitored at 235 nm. These measurements were carried out with spectropolarimeter Jasco J-815 using a 1 mm path-length cuvette. The temperature was controlled with a Peltier block and the measurements were performed at scan rate of 1.5 °C/min. In all conditions, protein concentration was 30 μM. Measurements were performed in 20 mM HEPES, pH 7.8, in the absence and in the presence of the corresponding salt concentrations.

Thermal denaturation was analyzed by fitting experimentally obtained data according to the following equation:

$$y_{obs} = \frac{y_N + y_D \exp\left[\frac{\Delta H_{vH}}{R}\left(\frac{1}{T} - \frac{1}{T_{trs}}\right)\right]}{1 + exp\left[\frac{\Delta H_{vH}}{R}\left(\frac{1}{T} - \frac{1}{T_{trs}}\right)\right]} \qquad (3)$$

where y_{obs} is experimentally measured parameter, y_N is the value of measured parameter for native state, y_D is the value of measured parameter for denaturated state, ΔH_{vH} is the van´t Hoff enthalpy change, R is the gas constant and T_{trs} is the transition temperature.

Differential scanning calorimetry (DSC). DSC measurements were performed using a VP-Capillary DSC system (Microcal Inc., acquired by Malvern Instruments Ltd.). The enzyme was dialyzed against 20 mM HEPES, pH 7.8. The enzyme in 1 M salt solutions was prepared by mixing 20 mM HEPES, pH 7.8 and corresponding 1.2 M salt in 20 mM HEPES, pH 7.8. The protein concentration in all measurements was 30 μM. All samples were degassed prior to measurement. The samples were heated from 25°C to 70°C with a scan rate of 1.5 °C/min. Thermograms were corrected by subtraction of the so-called chemical

baseline, i.e., the sigmoidal curve connecting the signal of excess heat capacity of the native and denatured states and normalized to the molar concentration of the protein.

2.6. Molecular dynamics simulations.

For performing the molecular dynamics (MD) simulations, AMBER99SB-ILDN protein and AMBER94 [33] were used. To build the initial structure, the HRV 3C protease was placed in the center of the cubic box with the size of 8×8×8 nm^3. A total number of 308 pair of cations and anions were added randomly by Packmol package in the simulation boxes [34,35] to reach the desired 1 M salt concentrations from the experiment. Then, the box is solvated by water molecules, using the TIP3P model of water [36]. As certain undesirable interactions might arise in the systems due to the randomly added molecules to the simulation box, the steepest descent minimization approach was utilized to eliminate all unfavorable interactions. After that, all systems were equilibrated by performing 100 ps NVT (Canonical ensemble) restrained simulations followed by 100 ps NPT (isothermal–isobaric ensemble). Equilibration proceeded with the production runs where the linear constraint solver (LINCS) algorithm [37] was employed for all bonds involving hydrogen atoms and short-range non-bonded interactions were cut off by 1.2 nm. Long-range electrostatic interactions were treated by the particle mesh Ewald method procedure [38]. To produce initial velocities, Maxwell–Boltzmann distribution was used for all simulations. V-rescale coupling algorithm was used [39] with the coupling constant of 0.1 ps to ensure constant temperature and pressure during the simulations. MD production runs were performed for 100 ns at 300K where 2 fs time step was used. Data for further analysis were stored in every 5 ps for all simulations. Gromacs 2018 program package was used for performing MD simulations [40–43]. Also, Visual Molecular Dynamics (VMD) [44] and PyMOL [45] was applied for visualizations and preparation of snapshots.

After the simulation, the root mean square deviation (RMSD) was calculated to show the structural fluctuations which can be associated to biological function. In this study, the RMSD is computed on C-alpha atoms to show the deviations of the backbone atoms of the enzyme from its initial structure and represents how structures and parts of structures alter over time as compared to the starting point (crystal structure, pdb code; 2B0F). Additionally, the root mean square fluctuation (RMSF) analysis was done to compute the fluctuations of each subset of the structure (residue) relative to the average structure of the simulation to show the average deviation of a residue over time from a reference position [46]. Furthermore, the number of hydrogen bonds with time was calculated based on geometric the criteria; the distance of donor−acceptor (which in Gromacs is 3.5 Å) and the angle between

hydrogen−donor−acceptor (which is 30°). In addition, a radial distribution function (RDF) was calculated to investigate the distribution of one molecule or an atom around one specific molecule or atom. Moreover, the electrostatic potential surface around protein by using Adaptive Poisson-Boltzmann Solver (APBS) software package was calculated [47].

3. Results

3.1 Effect of pH on the conformation and activity of HRV 3C protease

Despite an existence of several works describing properties of HRV 3C protease [21–23,27], there are no published data regarding its pH dependence of the catalytic activity, k_{cat}, and of stability, represented by ellipticity in the far-UV spectral region. This information is important for determination of the pH value suitable for more detailed analysis regarding the properties of the enzyme, which are addressed in this work. Results of such experiments are

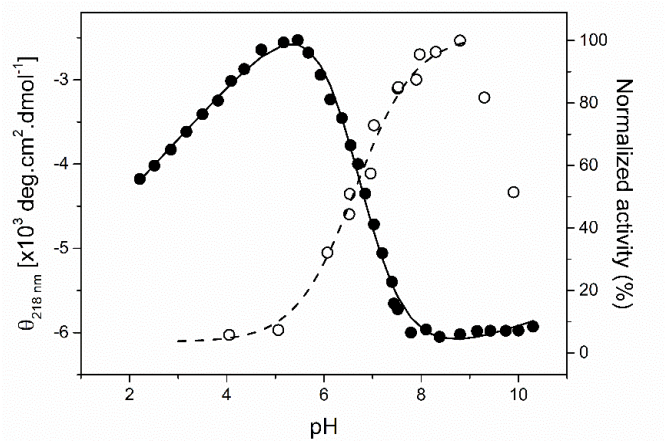

Figure 1. Dependence of ellipticity of HRV 3C protease measured in the far-UV region at 218 nm on pH. Fit to the catalytic activity and the ellipticity dependence according to the Equation 2 resulted in parameters of pK_a=6.7±0.1 and 6.6±0.1 and the value *n* equaled 0.80±0.10 and 0.85±0.09, respectively.

summarized in the Figure 1. Both the catalytic activity of 3C protease and ellipticity at 218 nm undergo sigmoidal transition, described by the Equation 2, with pK_a values about 6.65±0.15 with the *n* value ~0.83, suggesting a participation of one proton in the transition. Ellipticity reaches the maximal values at pH>7.8. Acidification of the solution leads to the decrease of ellipticity reaching the minimum at pH~5.3. Further pH decrease shows regaining of ellipticity, possibly as a result of a formation of moltenglobule-like form. The catalytic activity of HRV 3C protease shows analogous sigmoidal transition, the catalytic activity reaches the maximum in the pH region from pH 8 to pH 9, and the acidification of the enzyme solution leads to enzyme inhibition at pH<5. Increasing of pH above pH~9

negatively affects the enzyme activity as it is reflected by its steep decrease by 50% upon pH increase from pH 9 to pH 10. Based on the suggested catalytic mechanism [29,48], the k_{cat} increase with pK_a~6.6 likely corresponds to pK_a value of His40 residue in the active site. Analogous pH profile in the case of 3C-like proteinase from SARS coronavirus with different substrate TSALVQ-pNA [48] supports this conclusion. It needs to be noted that a type of buffer at given pH has no effect on the enzyme activity, i.e. in 20 mM of structurally different buffers such as Tris, MOPS or HEPES at pH 7.8, the enzyme activity was identical within an experimental error. However, previously it was shown that buffer type can significantly affect conformational stability of proteins [49] or intermolecular interactions [50]. Therefore, for more general conclusion of the independence of the HRV 3C protease properties on buffer type one would need to perform more methodical analysis. This result is in accordance with conclusion of Ullah et al. [23] that HRV 3C protease activity is relatively independent in various buffers. For further analysis of properties of 3C protease, we chose pH 7.8, because at this pH both ellipticity and activity of the enzyme reach the maximal values. The results presented in Figure 1 suggest that even pH up to ~9 might represent suitable experimental conditions for the enzyme analysis, but due to an increased tendency of 3C protease to aggregate at pH 8-9, likely as a result of closeness of its pI value ~8.5, we picked pH 7.8.

3.2 Specific effect of salts on catalytic properties of 3C protease

In the following, we analyzed the effect of 1 M sodium salts: sulfate, phosphate, chloride, bromide and perchlorate, on catalytic properties of 3C protease (Figure 2). One can

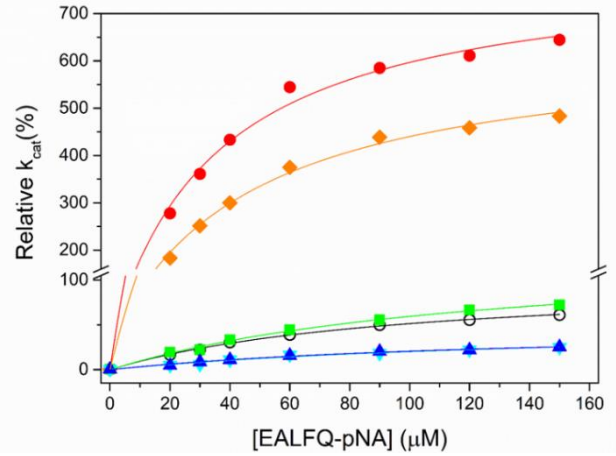

Figure 2. Michaelis-Menten plot of HRV 3C protease measured in the 20 mM HEPES, pH 7.8 (empty circles) and in the presence of 1M salts: Na_2SO_4 (red circles), Na_2HPO_4 (orange triangles), NaCl (green rectangulars), NaBr (cyan reverse triangles), and $NaClO_4$ (blue triangles). The solid lines correspond to the fits to the Michaelis-Menten equation (Equation 1). Presented dependences show unusual activation of 3C protease by kosmotropic salts.

notice a significant activation of the enzyme in the presence of kosmotropic salts, sulfate and phosphate, very small effect of sodium chloride and inhibition effect of chaotropic sodium salts, bromide and perchlorate. In the buffer, the values of parameters such as catalytic rate constant (k_{cat}), Michaelis constants (K_M) and catalytic efficiency (k_{cat}/K_M) were 0.0042±0.0002 s^{-1}, 98.2±0.1 μM, and 424±37 $M^{-1}s^{-1}$, respectively. Detailed analysis of the enzyme catalytic properties was also performed in dependence on salt concentration (Figure S1, Figure 3). For better comparison, we use the normalized values of the parameters related to the parameters obtained in the buffer in the absence of salts. The obtained parameters for

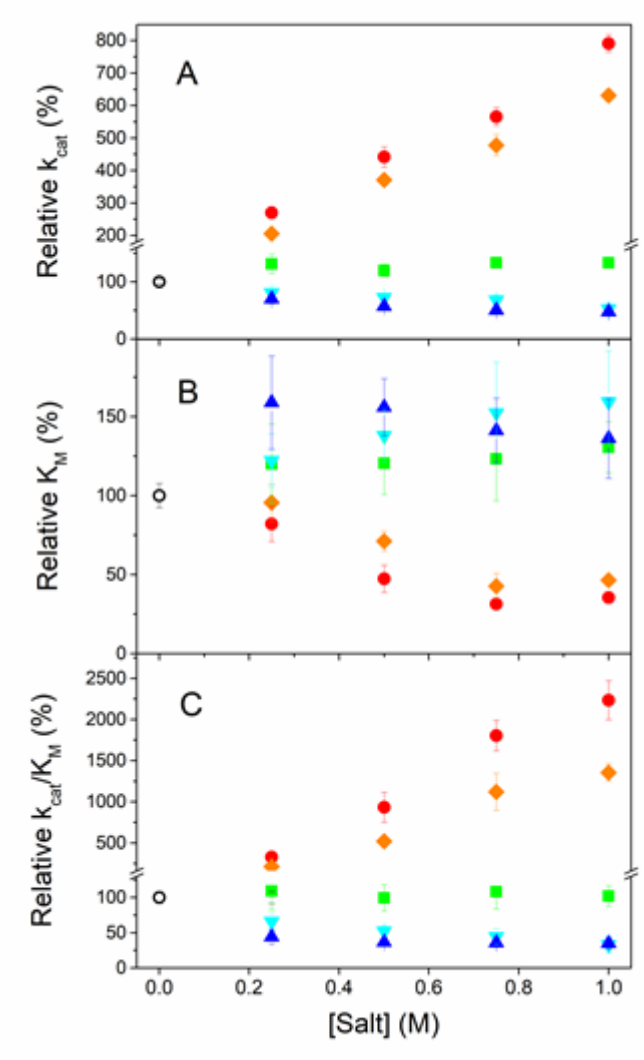

Figure 3. Dependences of parameters of k_{cat}, K_M, and k_{cat}/K_M obtained from Michaelis-Menten plots for HRV 3C protease measured in the 20 mM HEPES, pH 7.8 (empty circles) and in the presence of 0.25 M, 0.5 M, 0.75 M, and 1.0 M salts: Na_2SO_4 (red circles), Na_2HPO_4 (orange triangles), NaCl (green rectangulars), NaBr (cyan reverse triangles), and $NaClO_4$ (blue triangles). Presented plots clearly show dependence of the studied parameters on salt position in Hofmeister series and its concentration. The parameters were normalized to the values obtained in the buffer in the absence of salts: k_{cat}=0.0042 s^{-1}, K_M=98.2 μM and k_{cat}/K_M=424 $M^{-1}s^{-1}$.

all salts and corresponding concentrations are summarized in Table S1.

Dependences of the enzyme activity were fitted into Michaelis-Menten equation (Equation 2) and the obtained results shows that the effect of the studied salts on the catalytic properties is concentration dependent in a steadily manner. Kosmotropic salts significantly increase the values of k_{cat}, sulfate ~8x and phosphate ~6x, and in the presence of 1 M of both kosmotropic salts the values of K_M decrease ~3x. The combination of these changes in the catalytic efficiency lead to ~24x and ~15x increase of this parameter for HRV 3C protease in the presence of 1 M sodium sulfate and sodium phosphate, respectively. In the presence of 1 M sodium chloride, the catalytic properties of 3C protease are comparable with those at the low ionic strength. On the other hand, about 2x decrease of the values of k_{cat} and ~1.5-fold increase of the values of K_M was observed at 1 M concentration of the chaotropic salts.

3.3 Specific effect of salts on conformation and stability of HRV 3C protease

Such activation effect of 1 M kosmotropic salts on catalytic properties of enzymes is quite unusual, therefore we were interested how are affected the conformation and stability HRV 3C protease in the presence of 1 M salts. The secondary structure has been analyzed by CD in the far-UV spectral region and the tertiary structure by CD in the near-UV region and fluorescence of tyrosines (Figure 4). Chaotrope $NaClO_4$ had only minimal effect on the enzyme concentration but with an increased kosmotropic nature of anions the effect on the conformation became more distinguished. In the presence of 1 M Na_2SO_4 ellipticity in the far-UV region increased by ~10% when compared with the ellipticity of the enzyme in the buffer. More pronounce effect was observed in the ellipticity in the near-UV region in the presence of 1 M Na_2SO_4, which increased by ~40% and in tyrosine fluorescence, which decreased by ~40% in comparison with these parameters of the enzyme in the buffer. Observed changes of the CD spectra in the far-UV and near-UV regions as well as from tyrosine emission spectra suggest relatively small conformational changes in the secondary structure of 3C protease but quite significant change in the conformation of the level of its tertiary structure. The character of the changes, i.e. quantitative change in the amplitude of the parameters without their qualitative modification, suggest that the salt-induced changes do not generate a different conformation but more likely affect compactness/dynamics of the polypeptide chain. Modulation in dynamics of polypeptide chain of the enzyme should also pronounce in its stability.

Measurements of thermal stability of 3C protease in the presence of 1 M salts and in the absence of salts were performed by CD in the far-UV region at 218 nm and by DSC (Figure 5). Thermal transition at all conditions were irreversible, i.e. the re-heating of

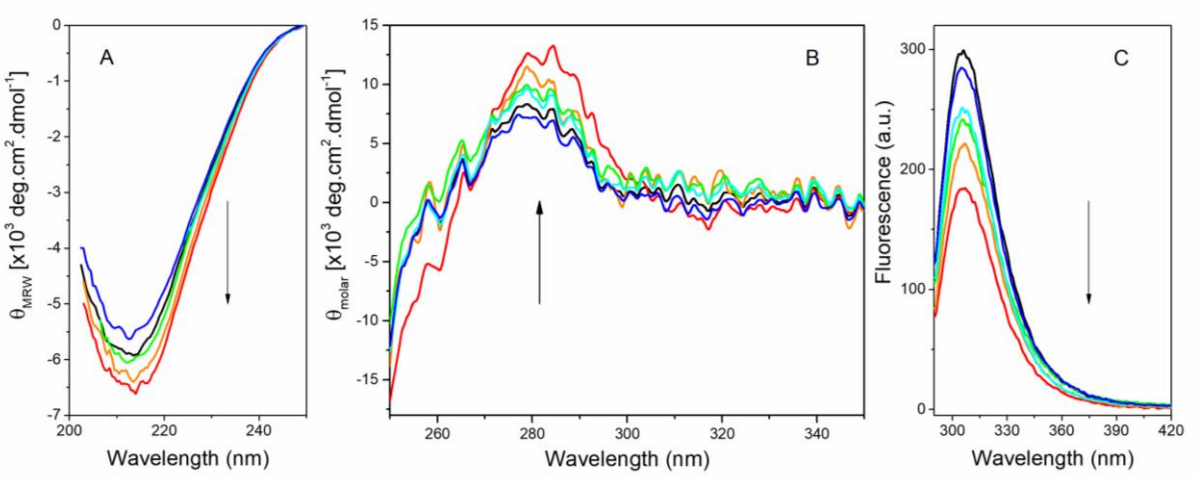

Figure 4. Effect of 1 M salts on CD spectrum of HRV 3C protease in the far-UV (A) and the near-UV (B) and on the tyrosines fluorescence (C). Presented results show that salts affect the enzyme conformation in a way that correlates with the Hofmeister effect. The arrows indicate dependence in the direction from chaotropic to kosmotropic salts. Color coding as in the previous figures: 20 mM HEPES, pH 7.8 (black), Na_2SO_4 (red), Na_2HPO_4 (orange), NaCl (green), NaBr (cyan reverse), and $NaClO_4$ (blue).

samples, which underwent thermal denaturation, showed no transition. Therefore, the obtained parameters from the thermal transitions can be considered as apparent parameters. In the effort to compare transition parameters of the enzyme in the presence of salts, all measurements were performed at the same protein concentration, 30 μM, and at the same heating rate, 1.5 °C/min. Both methods, CD at the far-UV region monitoring the stability of the secondary structure and DSC monitoring the stability of tertiary structure of 3C protease, led to nearly identical values of T_{trs}, CD/DSC: buffer, 50.5/50.4 °C; 1 M salts, Na_2SO_4, 58.6/59.2 °C, Na_2HPO_4, 57.0/56.8 °C, NaCl, 52.0/52.1 °C, NaBr, 51.0/51.3 °C, and $NaClO_4$, 44.8/43.1 °C. These results suggest that: (i) HRV 3C protease unfolds in two-state manner and (ii) the stabilization effect correspond to the position of anions in the Hofmeister series. For obtaining the parameter $dT_{trs}/d[salt]$ that in accordance with our experiences [4,51] is the best parameter for assessing de/stabilization effect of salts, we determined transition temperatures at four different concentrations of salts by CD. Obtained dependences of T_{trs} on salt concentration are linear and the slopes of the dependences corresponding to the parameter $dT_{trs}/d[salt]$ are listed in Table S2.

3.4 Correlation between parameters characterizing of HRV 3C protease and inherent properties of anions

There are numerous parameters, which describe specific properties of ions. Finding correlations between such inherent parameters of ions and the parameters characterizing functional and/or structural parameters that such ions modulate might be helpful for understanding of the Hofmeister effect. Inherent ion parameters that are often used for Hofmeister effect description are charge density, surface tension, air/water partition

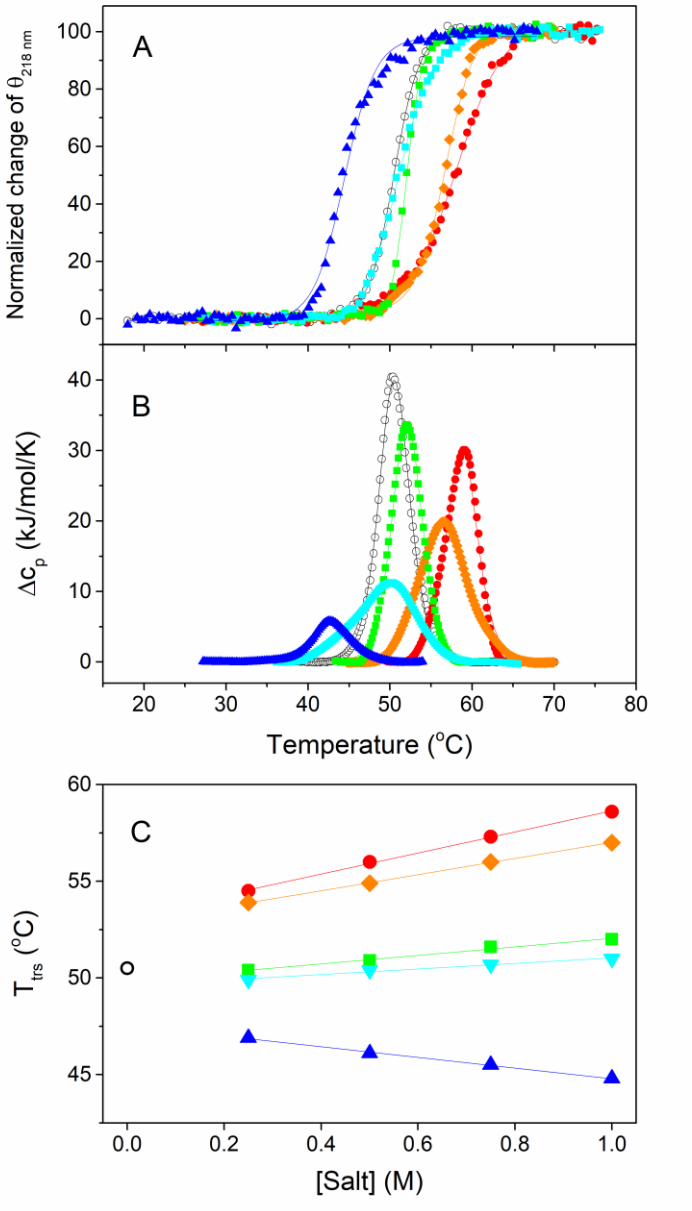

Figure 5. Effect of 1 M salts on HRV 3C protease thermal stability was studied by CD (A) and DSC (B). Transition temperatures of HRV 3C protease in dependence on salts concentration were obtained from CD (C). The slopes of linear dependences determine the parameters $dT_{trs}/d[salt]$. Color coding as in the previous figures: 20 mM HEPES, pH 7.8 (empty circles), Na_2SO_4 (red circles), Na_2HPO_4 (orange triangles), NaCl (green rectangulars), NaBr (cyan reverse triangles), and $NaClO_4$ (blue triangles). The solid lines in the boxes A and B correspond to the fits of two-state transition.

coefficient, viscosity B-coefficient, and partition coefficient at hydrocarbon surface or polar amide surface providing thus vast amount of combinations [4,51]. However, many of these parameters correlate between each others and thus significantly reduce a number of meaningful correlations. For example, the properties such as charge density, surface tension and air/water partition coefficient correlate between each other as well as Jones-Dole B viscosity coefficient and partition coefficient at hydrocarbon surface (Figure S2). The Jones-Dole B viscosity coefficient can be obtained from the equation for relative viscosity (η/η_0), which stands as $\eta/\eta_0=1+Ac^{1/2}+Bc$, where c is salt concentration and the A term depends on the interionic forces and the B term depends on ion-solvent interactions [52]**.** Taking this into account, we found out a close correlation between the de/stabilization effect of salts on the enzyme expressed as the parameter $dT_{trs}/d[salt]$ and the charge density of the anions (Figure 6A) and the salt effect on functional parameter of the enzyme, k_{cat}, and the viscosity B-coefficient (Figure 6B). Although we studied the effect of five sodium anions, we show only correlations for four anions, excluding phosphate anions for which we were unable to find the values of the corresponding parameters.

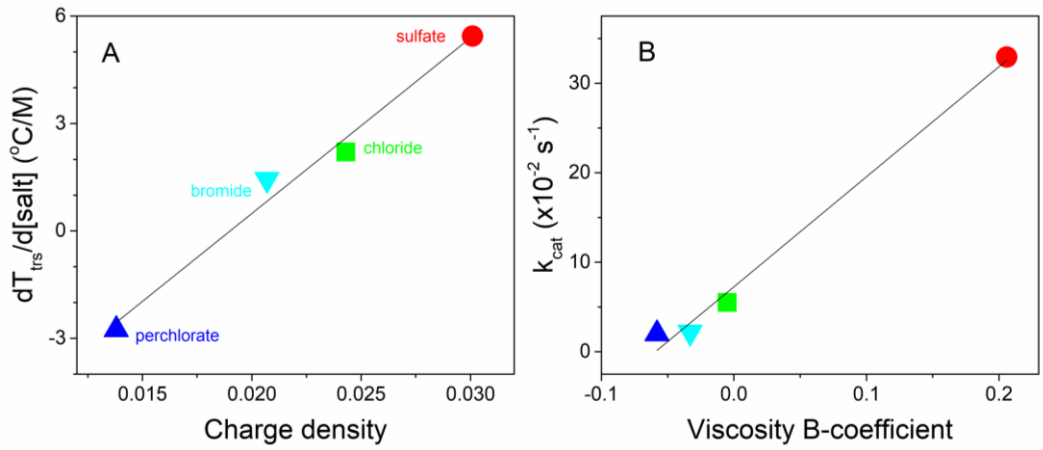

Figure 6. Correlations between selected experimentally determined parameters for HRV 3C protease and intrinsic parameters of the studied anions.

3.5 Correlation between parameters characterizing of HRV3C protease in the presence of salts

We were interested in whether there is a correlation between parameters characterizing catalytic and conformational properties of HRV 3C protease modulated by salts. Such interrelations might be helpful in identifying their potential causal

interrelationship. We found out correlations between several such parameters of HRV 3C protease affected by the salts: (i) parameters related to catalytic properties, k_{cat} and K_M (correlation coefficient R^2=0.9686), (ii) catalytic and conformational properties (excluding the parameter for the enzyme in 1 M $NaClO_4$), k_{cat} and $d[T_{trs}]/d[salt]$ (correlation coefficient R^2=0.9803). We would like to note that analogous correlation one can obtain by plotting $d[k_{cat}]/d[salt]$ vs $d[T_{trs}]/d[salt]$, and (iii) parameters characterizing conformational properties

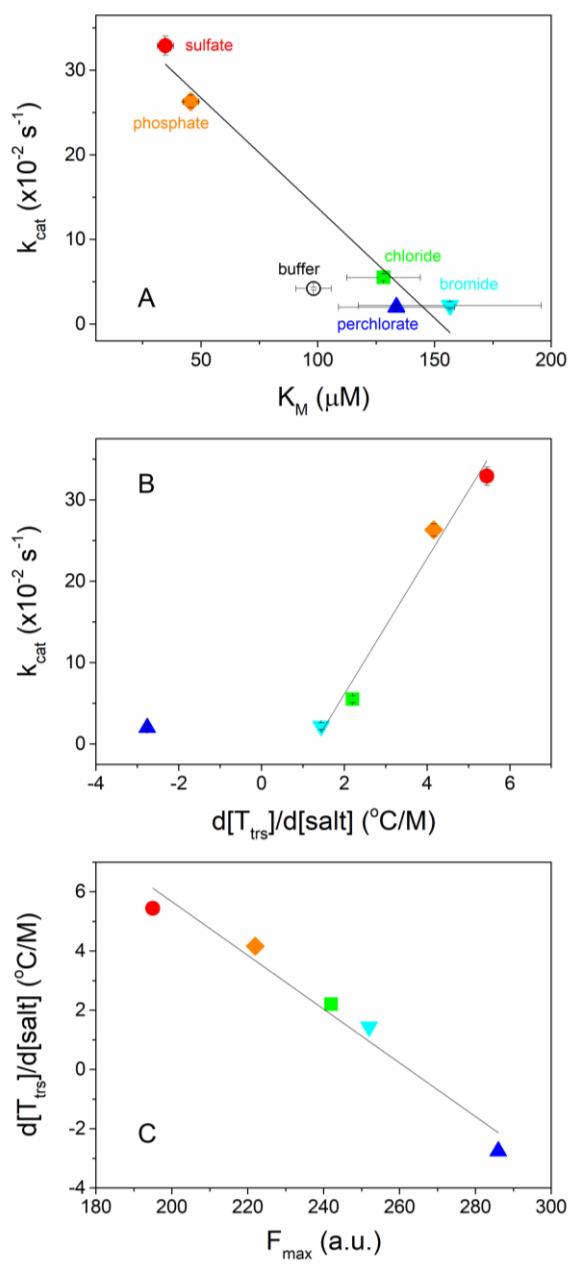

Figure 7. Correlations between selected experimentally determined parameters suggesting an interrelation of corresponding parameters. The data point corresponding to the buffer (A) and the outlier (B), corresponding to parameters obtained for 1 M $NaClO_4$, were not included into the correlations.

of the enzyme, de/stabilization parameter $d[T_{trs}]/d[salt]$ and parameter related to the enzyme conformation - maximum of tyrosine fluorescence emission (correlation coefficient R^2=0.9632). The correlations (i) and (ii) suggest tendency that more stable enzyme perform better in the catalysis and at the same time that more stable enzyme is characterized by smaller K_M values. The correlation (iii) indicates an existence of simple descriptor of the enzyme stability, which is proportional to intrinsic tyrosine fluorescence of the enzyme.

3.5 Molecular simulation (RMSD and RMSF) of HRV 3C protease in the presence of salts

The stability of the protein backbone along the simulation trajectories (100 ns) in aqueous solution and aqueous solution containing 1 M solution of selected salts: kosmotropic Na_2SO_4, neutral (from the point of view of Hofmeister effect) NaCl and chaotropic $NaClO_4$ were investigated by the root mean square deviation (RMSD) (Figure 8). Obtained results clearly show that the protein backbone solvated in aqueous solutions of Na_2SO_4 has much

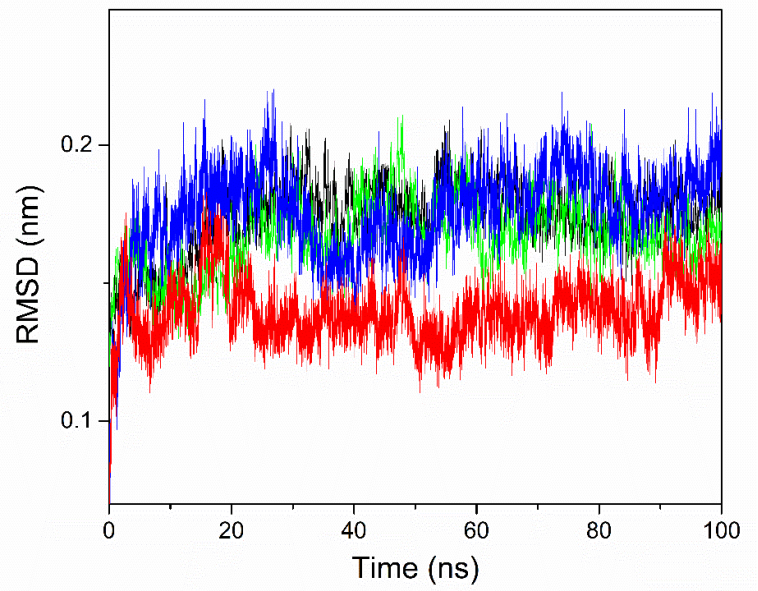

Figure 8. RMSD of HRV 3C protease solvated in pure water (black) and in the aqueous solution of Na_2SO_4 (red), NaCl (green) and $NaClO_4$ (blue) at concentration of 1M.

smaller values in comparison to the RMSD values of the protein backbone in water and in aqueous solution of NaCl and $NaClO_4$. More detailed comparison reveals that the RMSD values in the presence of NaCl are in average smaller than RMSD values of the protein backbone in water and $NaClO_4$. This observation is in consent with the Hofmeister effect and enables to rank anion ability to rigidity of the protein backbone in the order (from most to least rigidifying conditions): sulfate>chloride>perchlorate~water.

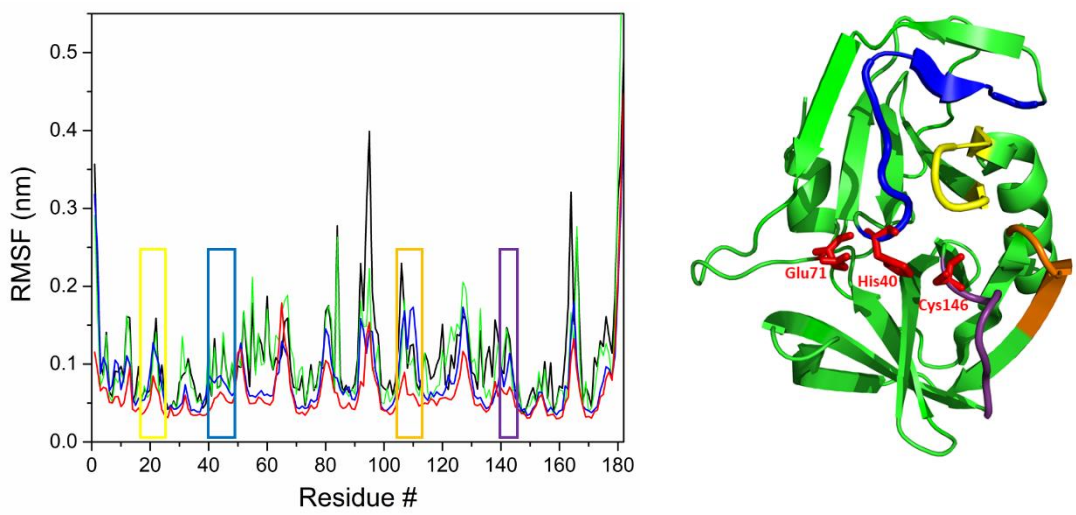

Figure 9. RMSF of HRV 3C protease (left) solvated in pure water (black) and in the aqueous solution of Na_2SO_4 (red), NaCl (green) and $NaClO_4$ (blue) at concentration of 1M. Rectangulars designate the regions of the polypeptide chain affected mainly by sulfates. Right: Structure of HRV 3C protease (2B0F.pdb) with highlighted regions, which flexibility was the selectively affected by sulfate anions: #18–25 (yellow), #40-50 (blue), #105-113 (orange), and #140-146 (violet).

A more detailed picture of the difference in the flexibility or stability of residues, within the simulation can be obtained from the root mean square fluctuation (RMSF) plot along the trajectory. In this study, the RMSF of each residue of HRV 3C protease was calculated to investigate the flexibility of residues to investigate the conformational changes upon the binding of anions. Figure 9 shows the RMSF of all residues of HRV 3C protease solvated in water and in 1 M aqueous solutions of Na_2SO_4, NaCl and $NaClO_4$. HRV 3C protease residues in the aqueous solution of Na_2SO_4 have fewer fluctuations as compared to the water or in the presence of sodium chloride. There are several regions of which fluctuation is significantly decreased in the presence of sodium sulfate: aa#18-25, aa# 40-50, aa#55-63, aa#69-78, aa#82-86, aa#105-113, and aa#140-146. It is not surprising that the regions containing the residues of the catalytic triad, Hi40-Glu71-Cys146, are part of the more rigid regions in the presence of sulfate. However, among listed parts of the polypeptide chain there are also regions, such as #55-63, #82-86, and surprisingly also the region #69-78 containing the residue of the catalytic triad, Glu71, that becomes less flexible in the presence of perchlorate. In Figure 9, there highlighted the regions of which flexibility is decreased selectively only in the presence of sulfates. Interestingly, the affected structural elements are mostly represented by loops or unstructured region.

The important region, residues 140–146, is located in the flexible loop (133-146) around the active site of HRV 3C protease. This loop involved in recognition of the P1/P2 residues of the substrates, in nucleophilic attack on the scissile bond, and play role in stabilization of the catalytic transition state [21,25,53]. In order to investigate the specific interactions of 3C protease with anions, the number of hydrogen bonds, lifetimes, and interaction energy of specific sites of 3C protease with anions in aqueous solution of Na_2SO_4, NaCl, and $NaClO_4$ were calculated. The number of hydrogen bonds formed between anions (sulfate and perchlorate) and amino acids in flexible loop containing amino acids 140-146 (Ala140, Thr141, Lys142, Thr143, Gly144, Gln145, Cys146), which are located in the part of the loop around the active site of the 3C protease, were analyzed in more detailed way. The results of the calculations show that the amino acids of the flexible loop form strong hydrogen bonds with sulfate and perchlorate anions (Table S3). From comparison of the lifetimes and energies associated with the hydrogen bonds of sulfate and perchlorate with amino acid residues in the loop 140-146 follows that: (i) sulfate anions interact only with certain amino acids (Lys142 and Thr 143), (ii) perchlorate anions interact with all amino acids of the loop, and (iii) interaction of sulfate with the corresponding amino acids is stronger than that of perchlorate anions.

4. Discussion

In this work we present the effect of sodium anions salts at increased (≥250 mM) concentration on properties of HRV 3C protease. We chose these conditions as anions at such concentrations significantly influence studied parameters of the enzymes and the high salt concentrations might have been of interest for biotechnological applications [17]. On the other hand, there are numerous example of the specific effect of cations on enzymes/proteins [54,55] even at close to physiological concentrations [13,56,57].

Modulation of HRV 3C protease properties by specific anion effect. Presented results show that the specific effect of anions on HRV 3C protease is concentration dependent and determined by their position in Hofmeister series. The effect of the studied anions on the stability and catalytic properties of HRV 3C protease can be accordingly ranked (from the most to the least effective) as follows: sulfate>phosphate>chloride>bromide>perchlorate. The analyzed enzyme properties depend on the position of anions in Hofmeister series in the monotonous way, i.e. from chaotropic perchlorate to kosmotropic sulfate (i) the stability of the enzyme, expressed in T_{trs}, increases, (ii) the catalytic rate, k_{cat}, steeply increases, (iii) the

Michaelis constant, K_M, decreases and negatively correlates with the k_{cat}, and their combination results in (iv) steep increase of the catalytic efficiency, k_{cat}/K_M (Figures 3, 5). The correlations between the intrinsic properties of anions and the properties of HRV 3C protease suggest that (i) stabilization effect of anions depends on the charge density of anions, and (ii) the catalytic properties of the enzyme is dependent on the viscosity B-coefficient of the anions (Figure 6). In our previous works, we showed for several independent proteins such as cytochrome *c*, apoflavodoxin, chymotrypsin and lysozyme a relation between charge density of anions and stability of the proteins [4,51,58].

We concluded that the unifying effect on different proteins must be related to the ion interaction with the peptide groups, which can be formally separated into two entities: the dehydrated, chaotropic amide group and the hydrated, kosmotropic carboxyl group [4]. This delineation of the peptide group provides a plausible explanation for the observed destabilization effect of chaotropic in comparison with kosmotropic anions on protein stability. In fact, dehydrated chaotropic anions should have greater affinity of for the dehydrated, chaotropic amide of the peptide group, than strongly hydrated kosmotropic anions surrounded by a thick hydration shell [4]. This conclusion goes along with the very recent work indicating the electrostatic origin of specific ion effects [59]. However, in the case of the catalytic properties a stronger correlation exists between the catalytic rate constant and the viscosity B-coefficient (Figure 6). Relation of the viscosity B-coefficients with the partition coefficients of anions on hydrocarbon surface (Figure S2) indicates interaction of anions with the hydrophobic patches on a protein surface. Enzyme activity is likely more sensitive to anion binding to the enzyme surface through weak dispersive interaction than the thermal stability of the enzyme. Several recent works suggest that in the specific ion effect plays a role besides the electrostatic interaction with peptide bond also electrostatic and hydrophobic interactions with side chains of amino acids and other parts of the polypeptide chain such as N-terminus and α-carbon [16,60–63]. This is in consent with recently developed model by Parson et al [64], which takes into account both properties of ions and (protein) interface [64,65]. The authors explain ion specificity as a result of the interplay of electrostatic and ion dispersion forces, which affect both physisorption and chemisorption at interfaces. Electrostatic physisorption is not ion-specific, but non-electrostatic physisorption is ion-specific. On the other hand, the major role in chemisorption plays polarizability of the ions. We showed previously that an existence of clear correlation of ion polarizability with protein properties in the corresponding salts depend on the proteins [51,58]. Thus, based on

this model, the type and strength of the interactions depend both on the nature of the ion (charge, size and polarizability) and that of interface (dielectric function, positions of specific interaction sites).

Based on literature data, enzymes affected by kosmotropic anions can be formally divided into three groups, the enzymes that are: (i) inhibited by salts [10,66,67], (ii) slightly activated, up to ~5-fold in the comparison with low ionic strength conditions [12,51,58,68,69], and (iii) activated more than ~5-fold in comparison with conditions without the salts [21,70–72]. The HRV 3C protease belongs into the last group. The question arises what property of HRV 3C protease, and other enzymes of this group, makes the enzyme so sensitive to kosmotropic anions? The one feature that distinguishes the enzymes of the last group from the groups (i) and (ii) is conformational change triggered by anions. In fact, while conformation of the enzymes of the groups (i) and (ii) are unaffected, modification of the enzyme conformation from the group (iii) can be identified by spectral parameters upon addition of kosmotropic salts. The change in the spectral parameters, accompanied by the enzyme stabilization, suggests that enzyme attains more folded (~10% increase in ellipticity in the far-UV spectral region) and more rigid conformation (~40% increase in ellipticity in the near-UV spectral region). Similar changes in conformations, suggesting more folded and more rigid state, are observed in the enzymes such as herpes simplex virus type I protease [70,71] and prostate specific antigen [72] of which activity is increased more than 100-fold in the presence of ~1 M kosmotropic salts. The issue of rigidity of the HRV 3C protease in the presence of salts has been addressed by MD simulations in 1 M salts: kosmotropic Na_2SO_4, neutral (from the point of view of Hofmeister series) NaCl, and chaotropic $NaClO_4$. The average RMSD values as a measure for conformational differences between the backbones of HRV 3C protease in kosmotropic Na_2SO_4 were the lowest in comparison with other conditions. The deviation of the enzyme backbone from the initial structure in Na_2SO_4 is smaller than other systems, which shows that the enzyme is more rigid and stable in the presence of the kosmotropic anions. In addition, the fluctuations of side chains of amino acids in the polypeptide chain regions containing aminoacids #18-25, #40-50, #105-113, and #140-146 becomes more rigid in the presence of only sulfate anions. Interestingly, increased rigidity of the same parts of the polypeptide chain, namely #105-113 and #140-146, has been observed upon complexation of the HRV 3C protease with certain rhinovirus inhibitors. This suggests a communication of these parts of the polypeptide chain on the protein surface with its active site [73]. Closer analysis of the loop 140-146 suggests that at least part of the decreased flexibility is due to the formation of stronger hydrogen bonds with doubly charged

sulfate anions. Interestingly, the regions that are specifically rigidified by sulfate anions are scattered over the whole enzyme structure. Thus, although we determined that in the presence of kosmotropic anions such as sulfate and phosphate HRV 3C protease becomes more stable and more rigid and consequently more efficient catalyst, the question arises why an increased rigidity of the certain and often remoted parts from the active site of polypeptide chain of enzyme makes it better catalyst.

Macromolecular rate theory. One plausible answer provides very recent theory so-called macromolecular rate theory (MMRT) [30]. The basis of MMRT is the observation that enzyme-catalyzed reactions occur with significant values of the activation heat capacity change, $\Delta c_p^{\ddagger}$, defined as the difference of the heat capacity between enzyme-transition complex and enzyme-substrate complex. In general, the value of $\Delta c_p^{\ddagger}$ is negative, the observation that is consistent with a classical description of enzyme catalysis, according which the enzyme binds more tightly the transition state than the substrate in its ground state. Experimental analysis showed that the major contribution to the heat capacity of folded protein in aqueous solvent is number of accessible vibrational modes [74], particularly low-frequency modes [75]. Prediction of $\Delta c_p^{\ddagger}$ for the catalyzed reaction of three distinct enzymes (ketosteroid isomerase, alpha-glucosidase, and Kemp eliminase) by atomic MD simulations revealed subtle dynamical changes such as tightening of loops around the active site along with changes in energetic fluctuations across whole enzyme [76,77]. Interestingly, analogous changes regarding rigidity of the loops around the active site, aminoacids 40-50 and 140-146, as well as decreased fluctuations at distant sites of the enzyme, aminoacids 18-25 and 105-113, have been observed in HRV 3C protease in the presence of sulfate anions. These changes in local and global flexibilities of the enzyme were indicated by MD simulations and indirectly by ellipticity and tyrosine fluorescence, suggest a change in the global enzyme fold.

In accordance with the MMRT the catalysis performed by HRV 3C protease in the presence of perchlorate and sulfate anions differs by the values $\Delta c_p^{\ddagger}$ assuming the identical transition state at both conditions. The value of $\Delta c_p^{\ddagger}$ is likely more negative in the perchlorate due to more flexible polypeptide chain of HRV 3C protease in the ground state. The more negative value of $\Delta c_p^{\ddagger}$ would, according to the MMRT, lead to higher curvature of k_{cat} dependence on temperature than for the conditions in the presence of sulfate and consequently to lower k_{cat} at studied temperature [30]. This explanation is in fact in the consent with observed activation of enzymes by kosmotropic salts, i.e. enzymes of both (ii)

and (iii) groups. On the other hand, there are enzymes, which are activated by chaotropic or neutral (from the point of view of Hofmeister effect) salts [10,78,79] in accordance with the hypothesis of a role of loosening of protein structure for a proper protein function [80,81]. These works are related to thermophilic enzymes measured well below their optimal temperature or the enzyme required for its function significant flexibility. At such conditions, as discussed by Arcus et al. [30], one has to take into consideration significant enthalpic effect with negative impact on catalytic properties. At these conditions, a destabilization of polypeptide chain by temperature and/or chaotropic agents as loosening factors of protein structure might be inevitable for an activation of such enzymes.

Conclusion

Analysis of the specific anion effect on properties of HRV 3C protease revealed their significant dependence on anions concentration and the position of anions in Hofmeister series: (i) Both functional properties of the enzyme, represented by parameters k_{cat} and K_M, and its conformational stability, represented by T_{trs} values, are clearly affected by Hofmeister effect. There is a strong correlation between increased in k_{cat} values and decrease in K_M values following anions ranking from chaotropes to kosmotropes. (ii) Increased stability of the enzyme in the presence of kosmotropic anions (sulfates and phosphates) is accompanied by anions-induced changes in the secondary and tertiary structures of the protein. (iii) Close correlation of the HRV 3C protease conformational stability with charge density of anions and its functional properties with the Jones-Dole B viscosity coefficient (correlating with partition coefficient at hydrocarbon surface) clearly points to the recent model regarding protein-ion interaction explaining it through physisorption and chemisorption, i.e. combined effect of electrostatic and dispersive forces. (iv) MD simulations indicate an increase of rigidity of certain parts of polypeptide chain in the presence of kosmotropic sulfate. Interestingly, similar parts of the enzyme loose flexibility upon binding of inhibitor suggesting thus a communication between the certain parts on the enzyme surface with residues in the active site. (v) Our results are in qualitative agreement with the macromolecular rate theory, which explains a modulation of catalytic properties of enzymes through modification of rigidity/flexibility of their polypeptide chain with direct effect on the transition state of the reaction.

CRediT authorship contribution statement

Eva Dušeková, Martin Berta, Dagmar Sedláková, David Řeha, Veronika Dzurillová, Anastasiia Shaposhnikova, Fatemeh Fadaei: Investigation, Formal analysis **Mária Tomková**: Writing – Review & Editing **Babak Minofar**: Conceptualization, Writing – Review & Editing **Erik Sedlák**: Funding acquisition, Formal analysis, Writing – Original Draft, Review & Editing.

Declaration of competing interest

None.

Acknowledgements

This work was supported by Slovak Research and Development Agency through the project APVV-20-0340 and by the grant agency of the Ministry of Education, Science, Research, and Sport of the Slovak Republic (grant no. VEGA 1/0074/22) and by the EU H2020-WIDESPREAD-05-2020 grant No. 952333, CasProt (Fostering high scientific quality in protein science in Eastern Slovakia).

References

[1] P.W. Fenimore, H. Frauenfelder, B.H. McMahon, F.G. Parak, Slaving: solvent fluctuations dominate protein dynamics and functions, Proc. Natl. Acad. Sci. U. S. A. 99 (2002) 16047–16051. https://doi.org/10.1073/PNAS.212637899.

[2] N. Prabhu, K. Sharp, Protein-solvent interactions, Chem. Rev. 106 (2006) 1616–1623. https://doi.org/10.1021/cr040437f.

[3] E. Brini, C.J. Fennell, M. Fernandez-Serra, B. Hribar-Lee, M. Lukšič, K.A. Dill, How Water's Properties Are Encoded in Its Molecular Structure and Energies, Chem. Rev. 117 (2017) 12385–12414. https://doi.org/10.1021/ACS.CHEMREV.7B00259.

[4] E. Sedlák, L. Stagg, P. Wittung-Stafshede, Effect of Hofmeister ions on protein thermal stability: roles of ion hydration and peptide groups?, Arch. Biochem. Biophys. 479 (2008) 69–73. https://doi.org/10.1016/J.ABB.2008.08.013.

[5] M.A. Metrick, G. MacDonald, Hofmeister ion effects on the solvation and thermal stability of model proteins lysozyme and myoglobin, Colloids Surfaces A Physicochem. Eng. Asp. 469 (2015) 242–251. https://doi.org/10.1016/j.colsurfa.2015.01.038.

[6] J. V. Schaefer, E. Sedlák, F. Kast, M. Nemergut, A. Plückthun, Modification of the kinetic stability of immunoglobulin G by solvent additives, MAbs. 10 (2018) 607–623. https://doi.org/10.1080/19420862.2018.1450126.

[7] S. Campioni, B. Mannini, J.P. López-Alonso, I.N. Shalova, A. Penco, E. Mulvihill, D. V. Laurents, A. Relini, F. Chiti, Salt anions promote the conversion of HypF-N into amyloid-like oligomers and modulate the structure of the oligomers and the monomeric precursor state, J. Mol. Biol. 424 (2012) 132–149. https://doi.org/10.1016/J.JMB.2012.09.023.

[8] P.J. Marek, V. Patsalo, D.F. Green, D.P. Raleigh, Ionic strength effects on amyloid formation by amylin are a complicated interplay among Debye screening, ion selectivity, and Hofmeister effects, Biochemistry. 51 (2012) 8478–8490. https://doi.org/10.1021/BI300574R.

[9] S. Poniková, A. Antošová, E. Demjén, D. Sedláková, J. Marek, R. Varhač, Z. Gažová, E. Sedlák, Lysozyme stability and amyloid fibrillization dependence on Hofmeister anions in acidic pH, J. Biol. Inorg. Chem. 20 (2015) 921–933. https://doi.org/10.1007/S00775-015-1276-0.

[10] G. Žoldák, M. Sprinzl, E. Sedlák, Modulation of activity of NADH oxidase from

Thermus thermophilus through change in flexibility in the enzyme active site induced by Hofmeister series anions, Eur. J. Biochem. 271 (2004) 48–57. https://doi.org/10.1046/J.1432-1033.2003.03900.X.

[11] H. Zhao, Effect of ions and other compatible solutes on enzyme activity, and its implication for biocatalysis using ionic liquids, J. Mol. Catal. B Enzym. 37 (2005) 16–25. https://doi.org/10.1016/j.molcatb.2005.08.007.

[12] A. Salis, D. Bilaničova, B.W. Ninham, M. Monduzzi, Hofmeister effects in enzymatic activity: weak and strong electrolyte influences on the activity of Candida rugosa lipase, J. Phys. Chem. B. 111 (2007) 1149–1156. https://doi.org/10.1021/JP066346Z.

[13] C. Carucci, F. Raccis, A. Salis, E. Magner, Specific ion effects on the enzymatic activity of alcohol dehydrogenase from Saccharomyces cerevisiae, Phys. Chem. Chem. Phys. 22 (2020) 6749–6754. https://doi.org/10.1039/C9CP06800G.

[14] M.G. Cacace, E.M. Landau, J.J. Ramsden, The Hofmeister series: salt and solvent effects on interfacial phenomena, Q. Rev. Biophys. 30 (1997) 241–277. https://doi.org/10.1017/S0033583597003363.

[15] P. Lo Nostro, B.W. Ninham, Hofmeister phenomena: an update on ion specificity in biology, Chem. Rev. 112 (2012) 2286–2322. https://doi.org/10.1021/CR200271J.

[16] A. Salis, B.W. Ninham, Models and mechanisms of Hofmeister effects in electrolyte solutions, and colloid and protein systems revisited, Chem. Soc. Rev. 43 (2014) 7358–7377. https://doi.org/10.1039/C4CS00144C.

[17] J. Yin, J.C. Chen, Q. Wu, G.Q. Chen, Halophiles, coming stars for industrial biotechnology, Biotechnol. Adv. 33 (2015) 1433–1442. https://doi.org/10.1016/J.BIOTECHADV.2014.10.008.

[18] S. Gault, M.W. Jaworek, R. Winter, C.S. Cockell, High pressures increase α-chymotrypsin enzyme activity under perchlorate stress, Commun. Biol. 3 (2020) 1–9. https://doi.org/10.1038/S42003-020-01279-4.

[19] A. Gendrin, N. Mangold, J.P. Bibring, Y. Langevin, B. Gondet, F. Poulet, G. Bonello, C. Quantin, J. Mustard, R. Arvidson, S. LeMouélic, Sulfates in Martian layered terrains: the OMEGA/Mars Express view, Science. 307 (2005) 1587–1591. https://doi.org/10.1126/SCIENCE.1109087.

[20] M.H. Hecht, S.P. Kounaves, R.C. Quinn, S.J. West, S.M.M. Young, D.W. Ming, D.C. Catling, B.C. Clark, W. V. Boynton, J. Hoffman, L.P. DeFlores, K. Gospodinova, J. Kapit, P.H. Smith, Detection of perchlorate and the soluble chemistry of martian soil at the Phoenix lander site, Science. 325 (2009) 64–67.

https://doi.org/10.1126/SCIENCE.1172466.

[21] Q.M. Wang, R.B. Johnson, Activation of human rhinovirus-14 3C protease, Virology. 280 (2001) 80–86. https://doi.org/10.1006/VIRO.2000.0760.

[22] I.E. Gouvea, W.A.S. Judice, M.H.S. Cezari, M.A. Juliano, T. Juhász, Z. Szeltner, L. Polgár, L. Juliano, Kosmotropic salt activation and substrate specificity of poliovirus protease 3C, Biochemistry. 45 (2006) 12083–12089. https://doi.org/10.1021/BI060793N.

[23] R. Ullah, M. Ali Shah, S. Tufail, F. Ismat, M. Imran, M. Iqbal, O. Mirza, M. Rhaman, Activity of the Human Rhinovirus 3C Protease Studied in Various Buffers, Additives and Detergents Solutions for Recombinant Protein Production, PLoS One. 11 (2016). https://doi.org/10.1371/JOURNAL.PONE.0153436.

[24] C. Liu, S. Boland, M.D. Scholle, D. Bardiot, A. Marchand, P. Chaltin, L.M. Blatt, L. Beigelman, J.A. Symons, P. Raboisson, Z.A. Gurard-Levin, K. Vandyck, J. Deval, Dual inhibition of SARS-CoV-2 and human rhinovirus with protease inhibitors in clinical development, Antiviral Res. 187 (2021) 105020. https://doi.org/10.1016/J.ANTIVIRAL.2021.105020.

[25] D.A. Matthews, W.W. Smith, R.A. Ferre, B. Condon, G. Budahazi, W. Slsson, J.E. Villafranca, C.A. Janson, H.E. McElroy, C.L. Gribskov, S. Worland, Structure of human rhinovirus 3C protease reveals a trypsin-like polypeptide fold, RNA-binding site, and means for cleaving precursor polyprotein, Cell. 77 (1994) 761–771. https://doi.org/10.1016/0092-8674(94)90059-0.

[26] M.G. Cordingley, P.L. Callahan, V. V. Sardana, V.M. Garsky, R.J. Colonno, Substrate requirements of human rhinovirus 3C protease for peptide cleavage in vitro, J. Biol. Chem. 265 (1990) 9062–9065. https://doi.org/10.1016/s0021-9258(19)38811-8.

[27] X. Fan, X. Li, Y. Zhou, M. Mei, P. Liu, J. Zhao, W. Peng, Z.B. Jiang, S. Yang, B.L. Iverson, G. Zhang, L. Yi, Quantitative Analysis of the Substrate Specificity of Human Rhinovirus 3C Protease and Exploration of Its Substrate Recognition Mechanisms, ACS Chem. Biol. 15 (2020) 63–73. https://doi.org/10.1021/ACSCHEMBIO.9B00539.

[28] K. Fan, L. Ma, X. Han, H. Liang, P. Wei, Y. Liu, L. Lai, The substrate specificity of SARS coronavirus 3C-like proteinase, Biochem. Biophys. Res. Commun. 329 (2005) 934–940. https://doi.org/10.1016/J.BBRC.2005.02.061.

[29] H. Wang, S. He, W. Deng, Y. Zhang, G. Li, J. Sun, W. Zhao, Y. Guo, Z. Yin, D. Li, L. Shang, Comprehensive Insights into the Catalytic Mechanism of Middle East Respiratory Syndrome 3C-Like Protease and Severe Acute Respiratory Syndrome 3C-

Like Protease, ACS Catal. 10 (2020) 5871–5890. https://doi.org/10.1021/ACSCATAL.0C00110.

[30] V.L. Arcus, E.J. Prentice, J.K. Hobbs, A.J. Mulholland, M.W. Van Der Kamp, C.R. Pudney, E.J. Parker, L.A. Schipper, On the Temperature Dependence of Enzyme-Catalyzed Rates, Biochemistry. 55 (2016) 1681–1688. https://doi.org/10.1021/ACS.BIOCHEM.5B01094.

[31] M. Nemergut, R. Škrabana, M. Berta, A. Plückthun, E. Sedlák, Purification of MBP fusion proteins using engineered DARPin affinity matrix, Int. J. Biol. Macromol. 187 (2021) 105–112. https://doi.org/10.1016/J.IJBIOMAC.2021.07.117.

[32] C.N. Pace, F. Vajdos, L. Fee, G. Grimsley, T. Gray, How to measure and predict the molar absorption coefficient of a protein, Protein Sci. 4 (1995) 2411–2423. https://doi.org/10.1002/PRO.5560041120.

[33] K. Lindorff-Larsen, S. Piana, K. Palmo, P. Maragakis, J.L. Klepeis, R.O. Dror, D.E. Shaw, Improved side-chain torsion potentials for the Amber ff99SB protein force field, Proteins. 78 (2010) 1950–1958. https://doi.org/10.1002/PROT.22711.

[34] J.M. Martínez, L. Martínez, Packing optimization for automated generation of complex system's initial configurations for molecular dynamics and docking, J. Comput. Chem. 24 (2003) 819–825. https://doi.org/10.1002/JCC.10216.

[35] L. Martínez, R. Andrade, E.G. Birgin, J.M. Martínez, Software News and Update Packmol: A Package for Building Initial Configurations forMolecular Dynamics Simulations, J. Comput. Chem. 30 (2009) 2157–2164. https://doi.org/https://doi.org/10.1002/jcc.21224.

[36] W.L. Jorgensen, J. Chandrasekhar, J.D. Madura, R.W. Impey, M.L. Klein, Comparison of simple potential functions for simulating liquid water | Browse - Journal of Chemical Physics, J. Chem. Phys. 79 (1983) 926–935. https://doi.org/https://doi.org/10.1063/1.445869.

[37] B. Hess, H. Bekker, H.J.C. Berendsen, J.G.E.M. Fraaije, LINCS: A Linear Constraint Solver for molecular simulations, J. Comput. Chem. 18 (1997) 1463–1472. https://doi.org/10.1002/(SICI)1096-987X(199709)18:12<1463::AID-JCC4>3.0.CO;2-H.

[38] T. Darden, D. York, L. Pedersen, Particle mesh Ewald: An N· log (N) method for Ewald sums in large systems, J. Chem. Phys. 98 (1993) 10089–10092. https://doi.org/https://doi.org/10.1063/1.464397.

[39] G. Bussi, D. Donadio, M. Parrinello, Canonical sampling through velocity rescaling, J.

Chem. Phys. 126 (2007) 014101. https://doi.org/10.1063/1.2408420.

[40] M.J. Abraham, T. Murtola, R. Schulz, S. Páll, J.C. Smith, B. Hess, E. Lindah, Gromacs: High performance molecular simulations through multi-level parallelism from laptops to supercomputers, SoftwareX. 1–2 (2015) 19–25. https://doi.org/10.1016/j.softx.2015.06.001.

[41] S. Pronk, S. Páll, R. Schulz, P. Larsson, P. Bjelkmar, R. Apostolov, M.R. Shirts, J.C. Smith, P.M. Kasson, D. Van Der Spoel, B. Hess, E. Lindahl, GROMACS 4.5: a high-throughput and highly parallel open source molecular simulation toolkit, Bioinformatics. 29 (2013) 845–854. https://doi.org/10.1093/BIOINFORMATICS/BTT055.

[42] B. Hess, C. Kutzner, D. Van Der Spoel, E. Lindahl, GROMACS 4: Algorithms for Highly Efficient, Load-Balanced, and Scalable Molecular Simulation, J. Chem. Theory Comput. 4 (2008) 435–447. https://doi.org/10.1021/CT700301Q.

[43] D. Van Der Spoel, E. Lindahl, B. Hess, G. Groenhof, A.E. Mark, H.J.C. Berendsen, GROMACS: fast, flexible, and free, J. Comput. Chem. 26 (2005) 1701–1718. https://doi.org/10.1002/JCC.20291.

[44] W. Humphrey, A. Dalke, K. Schulten, VMD: Visual molecular dynamics, J. Mol. Graph. 14 (1996) 33–38. https://doi.org/10.1016/0263-7855(96)00018-5.

[45] W.L. Delano, The PyMOL Molecular Graphics System, De-Lano Sci. 40 (2002).

[46] L. Martínez, Automatic identification of mobile and rigid substructures in molecular dynamics simulations and fractional structural fluctuation analysis, PLoS One. 10 (2015) e0119264. https://doi.org/10.1371/JOURNAL.PONE.0119264.

[47] F. Vascon, M. Gasparotto, M. Giacomello, L. Cendron, E. Bergantino, F. Filippini, I. Righetto, Protein electrostatics: From computational and structural analysis to discovery of functional fingerprints and biotechnological design, Comput. Struct. Biotechnol. J. 18 (2020) 1774–1789. https://doi.org/10.1016/J.CSBJ.2020.06.029.

[48] C. Huang, P. Wei, K. Fan, Y. Liu, L. Lai, 3C-like proteinase from SARS coronavirus catalyzes substrate hydrolysis by a general base mechanism, Biochemistry. 43 (2004) 4568–4574. https://doi.org/10.1021/BI036022Q.

[49] M.A. Metrick, J.E. Temple, G. Macdonald, The effects of buffers and pH on the thermal stability, unfolding and substrate binding of RecA, Biophys. Chem. 184 (2013) 29–36. https://doi.org/10.1016/J.BPC.2013.08.001.

[50] A. Salis, L. Cappai, C. Carucci, D.F. Parsons, M. Monduzzi, Specific Buffer Effects on the Intermolecular Interactions among Protein Molecules at Physiological pH, J. Phys.

Chem. Lett. 11 (2020) 6805–6811. https://doi.org/10.1021/ACS.JPCLETT.0C01900.

[51] K. Garajová, A. Balogová, E. Dušeková, D. Sedláková, E. Sedlák, R. Varhač, Correlation of lysozyme activity and stability in the presence of Hofmeister series anions, Biochim. Biophys. Acta. Proteins Proteomics. 1865 (2017) 281–288. https://doi.org/10.1016/J.BBAPAP.2016.11.016.

[52] H. Donald, B. Jenkins, Y. Marcus, Viscosity S-Coefficients of Ions in Solution, Chem. Rev. 95 (1995) 2695–2724. https://doi.org/10.1021/CR00040A004/ASSET/CR00040A004.FP.PNG_V03.

[53] T.C. Bjorndahl, L.C. Andrew, V. Semenchenko, D.S. Wishart, NMR solution structures of the apo and peptide-inhibited human rhinovirus 3C protease (Serotype 14): structural and dynamic comparison, Biochemistry. 46 (2007) 12945–12958. https://doi.org/10.1021/BI7010866.

[54] K. Tóth, E. Sedlák, M. Sprinzl, G. Žoldák, Flexibility and enzyme activity of NADH oxidase from Thermus thermophilus in the presence of monovalent cations of Hofmeister series, Biochim. Biophys. Acta. 1784 (2008) 789–795. https://doi.org/10.1016/J.BBAPAP.2008.01.022.

[55] V. Štěpánková, J. Paterová, J. Damborský, P. Jungwirth, R. Chaloupková, J. Heyda, Cation-specific effects on enzymatic catalysis driven by interactions at the tunnel mouth, J. Phys. Chem. B. 117 (2013) 6394–6402. https://doi.org/10.1021/JP401506V.

[56] L. Medda, A. Salis, E. Magner, Specific ion effects on the electrochemical properties of cytochrome c, Phys. Chem. Chem. Phys. 14 (2012) 2875–2883. https://doi.org/10.1039/C2CP23401G.

[57] L. Medda, C. Carucci, D.F. Parsons, B.W. Ninham, M. Monduzzi, A. Salis, Specific cation effects on hemoglobin aggregation below and at physiological salt concentration, Langmuir. 29 (2013) 15350–15358. https://doi.org/10.1021/LA404249N.

[58] E. Dušeková, K. Garajová, R. Yavaşer, R. Varhač, E. Sedlák, Hofmeister effect on catalytic properties of chymotrypsin is substrate-dependent, Biophys. Chem. 243 (2018) 8–16. https://doi.org/10.1016/J.BPC.2018.10.002.

[59] K.P. Gregory, E.J. Wanless, G.B. Webber, V.S.J. Craig, A.J. Page, The electrostatic origins of specific ion effects: quantifying the Hofmeister series for anions, Chem. Sci. 12 (2021) 15007–15015. https://doi.org/10.1039/D1SC03568A.

[60] K.B. Rembert, J. Paterová, J. Heyda, C. Hilty, P. Jungwirth, P.S. Cremer, Molecular mechanisms of ion-specific effects on proteins, J. Am. Chem. Soc. 134 (2012) 10039–

10046. https://doi.org/10.1021/JA301297G.

[61] J. Paterová, K.B. Rembert, J. Heyda, Y. Kurra, H.I. Okur, W.R. Liu, C. Hilty, P.S. Cremer, P. Jungwirth, Reversal of the hofmeister series: specific ion effects on peptides, J. Phys. Chem. B. 117 (2013) 8150–8158. https://doi.org/10.1021/JP405683S.

[62] H.I. Okur, J. Hladílková, K.B. Rembert, Y. Cho, J. Heyda, J. Dzubiella, P.S. Cremer, P. Jungwirth, Beyond the Hofmeister Series: Ion-Specific Effects on Proteins and Their Biological Functions, J. Phys. Chem. B. 121 (2017) 1997–2014. https://doi.org/10.1021/ACS.JPCB.6B10797.

[63] L. Zhao, S. Damodaran, Hofmeister Order of Anions on Protein Stability Originates from Lifshitz-van der Waals Dispersion Interaction with the Protein Phase, Langmuir. 35 (2019) 12993–13002. https://doi.org/10.1021/ACS.LANGMUIR.9B00486.

[64] D.F. Parsons, T.T. Duignan, A. Salis, Cation effects on haemoglobin aggregation: balance of chemisorption against physisorption of ions, Interface Focus. 7 (2017). https://doi.org/10.1098/RSFS.2016.0137.

[65] D.F. Parsons, A. Salis, A thermodynamic correction to the theory of competitive chemisorption of ions at surface sites with nonelectrostatic physisorption, J. Chem. Phys. 151 (2019). https://doi.org/10.1063/1.5096237.

[66] J.C. Warren, S.G. Cheatum, Effect of neutral salts on enzyme activity and structure, Biochemistry. 5 (1966) 1702–1707. https://doi.org/10.1021/BI00869A036.

[67] J.S. Nishimura, R. Narayanasami, R.T. Miller, L.J. Roman, S. Panda, B.S.S. Masters, The stimulatory effects of Hofmeister ions on the activities of neuronal nitric-oxide synthase. Apparent substrate inhibition by l-arginine is overcome in the presence of protein-destabilizing agents, J. Biol. Chem. 274 (1999) 5399–5406. https://doi.org/10.1074/JBC.274.9.5399.

[68] E.B. Kearney, B.A.C. Ackrell, M. Mayr, T.P. Singer, Activation of succinate dehydrogenase by anions and pH, J. Biol. Chem. 249 (1974) 2016–2020. https://doi.org/10.1016/s0021-9258(19)42789-0.

[69] Z. Yang, X.J. Liu, C. Chen, P.J. Halling, Hofmeister effects on activity and stability of alkaline phosphatase, Biochim. Biophys. Acta. 1804 (2010) 821–828. https://doi.org/10.1016/J.BBAPAP.2009.12.005.

[70] D.L. Hall, P.L. Darke, Activation of the herpes simplex virus type 1 protease, J. Biol. Chem. 270 (1995) 22697–22700. https://doi.org/10.1074/JBC.270.39.22697.

[71] G. Yamanaka, C.L. DiIanni, D.R. O'Boyle, J. Stevens, S.P. Weinheimer, I.C.

Deckman, L. Matusick-Kumar, R.J. Colonno, Stimulation of the herpes simplex virus type I protease by antichaeotrophic salts, J. Biol. Chem. 270 (1995) 30168–30172. https://doi.org/10.1074/JBC.270.50.30168.

[72] X. Huang, C.T. Knoell, G. Frey, M. Hazegh-Azam, A.H. Tashjian, L. Hedstrom, R.H. Abeles, N.S. Timasheff, Modulation of recombinant human prostate-specific antigen: activation by Hofmeister salts and inhibition by azapeptides. Appendix: thermodynamic interpretation of the activation by concentrated salts, Biochemistry. 40 (2001) 11734–11741. https://doi.org/10.1021/BI010364J.

[73] N.M. Buthelezi, K.E. Machaba, M.E. Soliman, The Identification of potential human rhinovirus inhibitors: exploring the binding landscape of HRV-3C protease through PRED pharmacophore screening, Https://Doi.Org/10.2217/Fvl-2017-0084. 12 (2017) 747–759. https://doi.org/10.2217/FVL-2017-0084.

[74] M.J. Seewald, K. Pichumani, C. Stowell, B. V. Tibbals, L. Regan, M.J. Stone, The role of backbone conformational heat capacity in protein stability: temperature dependent dynamics of the B1 domain of Streptococcal protein G, Protein Sci. 9 (2000) 1177–1193. https://doi.org/10.1110/PS.9.6.1177.

[75] J.L. Klepeis, K. Lindorff-Larsen, R.O. Dror, D.E. Shaw, Long-timescale molecular dynamics simulations of protein structure and function, Curr. Opin. Struct. Biol. 19 (2009) 120–127. https://doi.org/10.1016/J.SBI.2009.03.004.

[76] M.W. Van Der Kamp, E.J. Prentice, K.L. Kraakman, M. Connolly, A.J. Mulholland, V.L. Arcus, Dynamical origins of heat capacity changes in enzyme-catalysed reactions, Nat. Commun. 9 (2018) 1177. https://doi.org/10.1038/S41467-018-03597-Y.

[77] H.A. Bunzel, J.L.R. Anderson, D. Hilvert, V.L. Arcus, M.W. van der Kamp, A.J. Mulholland, Evolution of dynamical networks enhances catalysis in a designer enzyme, Nat. Chem. 13 (2021) 1017–1022. https://doi.org/10.1038/S41557-021-00763-6.

[78] H.J. Zhang, X.R. Sheng, X.M. Pan, J.M. Zhou, Activation of adenylate kinase by denaturants is due to the increasing conformational flexibility at its active sites, Biochem. Biophys. Res. Commun. 238 (1997) 382–386. https://doi.org/10.1006/BBRC.1997.7301.

[79] G. Žoldák, R. Šut'ák, M. Antalík, M. Sprinzl, E. Sedlák, Role of conformational flexibility for enzymatic activity in NADH oxidase from Thermus thermophilus, Eur. J. Biochem. 270 (2003) 4887–4897. https://doi.org/10.1046/J.1432-1033.2003.03889.X.

[80] P. Závodszky, J. Kardos, Á. Svingor, G.A. Petsko, Adjustment of conformational flexibility is a key event in the thermal adaptation of proteins, Proc. Natl. Acad. Sci. U. S. A. 95 (1998) 7406–7411. https://doi.org/10.1073/PNAS.95.13.7406.

[81] A. Dér, J.J. Ramsden, Evidence for loosening of a protein mechanism, Naturwissenschaften. 85 (1998) 353–355. https://doi.org/10.1007/s001140050515.